Vol. 14 (núm. 1) pp. 47-56
Enero-Junio 2023

Ciencia en Desarrollo
Revista de la Facultad de Ciencias
Vicerrectoría en Investigación y Extensión - VIE
Centro de Investigaciones y Extensión de la Facultad de Ciencias - CIEC

https://doi.org/10.19053/01217488.v14.n1.2023.14191

Characterization and Commissioning of a Triple-GEM Detector

Caracterización y comisionamiento de un detector Triple-GEM

Andrea Velásquez Moros[1] and Héctor Fabio Castro Serrato[2]

Abstract

We present in detail the characterization and commissioning of a triple Gas Electron Multiplier (triple-GEM) detector. The response to various sources of radiation was studied, and its efficiency, gain, energy resolution, and time resolution were calculated. We found an energy resolution of 19.5%, a time resolution of 40 ns., and a maximum gain of 5×10^6. We conclude that the detector can be confidently used in further studies of medical dosimetry, since it is working in the proportional mode.

***Keywords*:** Commissioning, Detector characterization, GEM detector, Particle detectors, Radioactivity, X-rays.

Resumen

Se presenta en detalle la caracterización y la puesta en funcionamiento de un detector triple multiplicador de electrones gaseoso (triple-GEM). Se estudió la respuesta a varias fuentes de radiación, y se calculó su eficiencia, ganancia, resolución energética y resolución temporal. Se encontró una resolución energética de 19.5 %, una resolución temporal de 40 ns. y una ganancia máxima de 5×10^6. Concluímos que el detector puede ser utilizado con confianza en estudios futuros sobre dosimetría médica, ya que su funcionamiento cae dentro de la región proporcional.

***Palabras clave*:** Caracterización de detectores, Comisionamiento, Detectores de partículas, Detectores GEM, Radiactividad, Rayos X.

Recepción: 5-abr-2022
Aceptación: 8-jun-2022

[1]M.Sc. Cryomag Research Group, Physics Department, Universidad Nacional de Colombia. Email: anvelasquezm@unal.edu.co
[2]PhD. Cryomag Research Group, Physics Department, Universidad Nacional de Colombia

1 Introduction

Fabio Sauli in 1996, at CERN, developed the Gas Electron Multiplier (GEM), in which the electrodes structure consists of micrometer-sized holes where their geometry bends and concentrates the electric field in such a way that a large amplification is achieved in comparison to other Micropattern Gas Detectors. The GEM detector allows for notably less aging of the gas mixture after large bouts of radiation, a wide variety of applications, mass production, flexible geometry, low noise, fast electronic signal, and improved spatial and time resolution [1].

Since the early 2000 s, there have been GEM detectors at multiple High Energy Physics facilities, such as the COMPASS [2], TOTEM [3], and LHCb [4] experiments. Additionally, GEM-based detectors replaced other gaseous devices with a limited rate capability, such as the muon detectors at CMS [5] and the end-caps of the time-projection chamber at ALICE, for neutron detection, fast tracking, and improved readout for large volume drift chambers [6]. They have also been proposed for the future International Linear Collider (ILC) [7] and the STAR [8] and PHENIX [9] experiments at the Relativistic Heavy Ion Collider (RHIC).

In this work we present in detail how this detector is characterized, calibrated, and commissioned. In a separate work we have studied the feasibility of using it for medical dosimetry [10].

A triple-GEM detector was acquired by the CRYOMAG research group at Universidad Nacional de Colombia from the RD51 collaboration at CERN, where it was fabricated, then assembled in a clean room by one of the authors. Later it was commissioned at the Cryomag laboratory at the National University of Colombia. The commissioning consisted on checking the correct operation of the detector, starting from its physical integrity, gas circuit, implementation of the electrical polarization network and signal generation circuit. The electrical characteristics were also determined, like the safe operating voltage range, gain, and energy calibration. These procedures will be explained thoroughly so that newcomers with particle detectors, in particular with GEM detectors, will get acquainted with these details.

2 Theoretical Background

2.1 Characteristic response curve

The characteristic response curve is a graph of voltage applied vs charge collected, which demonstrates the operating regions of gaseous ionizing detectors. Its general shape has been replicated elsewhere [11]. The proportional counter region (where voltage applied is proportional to charge in a logarithmic scale) is of particular interest for spectroscopy and dosimetry applications, since collected charge is proportional to the energy deposited by detected particles. A detailed discussion of each region can be found in [12].

2.2 Choice of gas

The filling gas needs to satisfy multiple requirements, including being ionized at low voltages, allow a high gain, have good proportionality, high rate capacity, and high ion mobility. These conditions are better satisfied with a mix of gases than with just one. To be ionized with a low voltage, the best options are noble gases [13]. This happens because noble gases can only be excited through the absorption and emission of photons [14]. Argon is the most commonly used due to its relatively low ionization energy of 15.76 eV., low cost, availability, and safety (hydrogen is flammable, and helium is expensive and scarce).

However, due to its low ionization energy, using pure argon allows gains of up to 10^3 to 10^4 before discharges and sparks start occurring. Mixing it with a second polyatomic gas can fix this problem. Some examples that work well are methane, alcohol, CO_2, and BF_3. Since they have a large amount of non-radiative excited states (such as vibrational and rotational), these molecules act as inhibitors (quenchers) by absorbing photons of all energies being radiated by the de-excitations of the noble gas atoms, which otherwise would extract photoelectrons from the cathodes that may produce secondary ionizations at multiple places inside the detector, reducing the spatial resolution [14]. Even a small percentage of quencher in the gas mixture may increase the gain up to 10^6. For GEM detectors, the most common gas mixture is between 10-30% carbon dioxide and 70-90% argon.

2.3 The Triple-GEM detector

GEM detectors consist of an anode, a cathode, and a GEM foil in between (see Figure 1). A GEM foil is a 50 µm thick insulating kapton layer covered with copper on both sides, and a grid of 50-100 holes per square millimeter perforated using laser techniques. The holes have a diameter of 70 µm, a separation of 140 µm, and a double-conical shape [15]. The anode is covered in a two-dimensional copper strip readout, which allows precise measurements of the location of an incoming particle. This structure is placed inside a tight box and filled with the gas mixture.

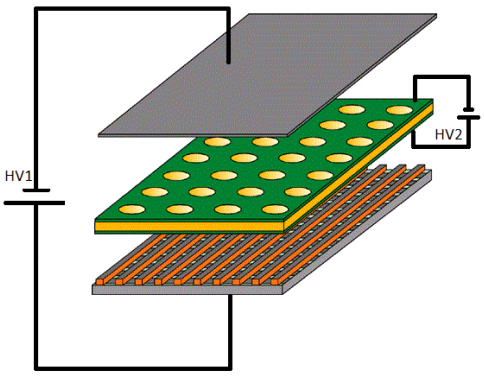

Figure 1. Schematic view of a single-GEM detector [16]. We see the cathode plane on top, the GEM perforated foil in the middle and the strip readout electrodes at the bottom. Appropriate high voltages are applied in order to drag and amplify generated charges in the electrodes. The anode structure is placed inside a sealed chamber and filled with the gas mixture.

High voltage (HV2) is applied between the two faces of the GEM foil, generating an electric field, as illustrated in Figures 1 and 2.

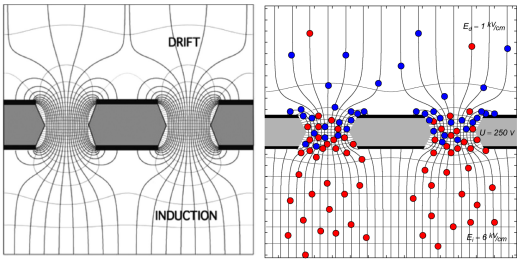

Figure 2. The electric field in the region of the holes of a GEM electrode [16][17]

When ionizing radiation such as photons or muons enters a GEM detector, ionizing the argon atoms, free electrons are created which drift towards the GEM foil following the electric field lines. They are guided inside the holes where the increased density of field lines gives them a large velocity such that after leaving the holes they acquire enough energy to ionize other gas atoms, creating electron multiplication. Thereafter, the electrons continue their trajectory onto the readout pane where a signal is detected.

With a single GEM foil, the gain is approximately 100 or 200 at about HV2 = 400 V [17]. However, GEM foils can be piled up on top of each other, forming double, triple, or even higher-level GEMs. Each gain is multiplied so, taking losses into account, a triple-GEM could provide a gain of 10^4 or 10^6 using relatively low voltages, thus reducing the chance of getting sparks and damaging the detector.

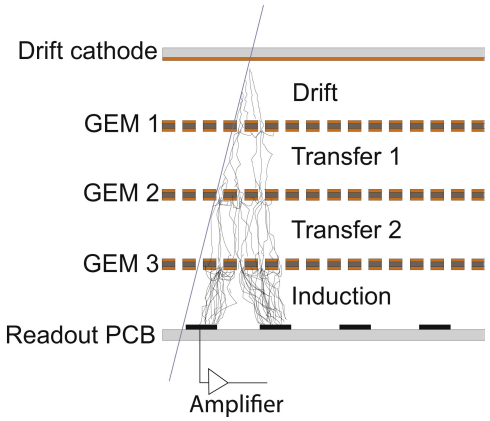

Figure 3. Drift, multiplication, and collection of charges in a triple-GEM detector [18]

3 Experimental setup and methodology

The detector was acquired from the CERN RD51 collaboration. It was assembled and first tested at the RD51 laboratory by one of the authors, under supervision and guidance of an RD51 specialist. The rest of the project was developed at the CRYOMAG Particle Detectors Laboratory at Universidad Nacional de Colombia.

The instruments used in this experiment were the triple-GEM detector, a NIM (Nuclear Instrument Module) standard module, a fast digital oscilloscope, a dual counter, a picoammeter, a Geiger-Müller detector, a gas supply system, and radioactive sources.

Figure 4. Fe-55 signal taken with the triple-GEM detector at a supply voltage of −4202 V. The horizontal time scale is 200 ns per division, and the vertical voltage scale is 2 mV per division.

- Triple-GEM detector: it includes a connection to a high voltage supply, gas input and output terminals, signal outputs located at the strips and at the bottom of the third GEM foil.

  The detector's 512 x 512 strips were connected together, obtaining a single signal for each detection. This configuration is useful for 1D dosimetry but limits the possibility of having two-dimensional spatial resolution.

- Operating gas: 75% argon and 25% carbon dioxide.

- Radioactive sources: Fe-55, Sr-90, Tl-204, and Am-241.

- Radiation detector Inspector EXP

The detector was first assembled inside a clean room at CERN's RD51 laboratory. The rest of the characterization was made at the Cryomag laboratory in Colombia. To check its functionality, all connections in the external voltage divider circuit were tested along with the voltages and current throughout it. Then detection signals were observed on the oscilloscope when the voltage was increased enough for the gas to be ionized by either muons from cosmic rays, an X-ray generator, or a radioactive source. Peak signals larger than the background noise indicated correct operation of the detector (see Figure 4).

Measurements were then taken for voltages ranging between −3700 V and −4575 V (the polarization voltage of the detector is negative) with an uncertainty of ±1 V in steps of 25 V, to find the range of operation. Measurements of counts vs. voltage were made to determine the efficiency and operating voltage range.

In order to do the characterization, typical signals for cosmic rays were studied using the oscilloscope. Parameters such as amplitude, duration, shape, and polarity of pulses were studied. The size of the background noise and range of operation before sparks appear was determined. Properties such as sensitivity, energy resolution, time resolution, efficiency, gain, and response to various sources were measured.

After characterization, the detector was calibrated by reproducing the spectrum of iron-55, which has a characteristic gamma emission line at 5.9 keV.

4 Results and analysis

An important issue for the correct operation of the particle detector is noise insulation. We used a flat tinned copper braid to ground all the electronic equipment and the triple-GEM detector. Without it, the electronic noise is so big that it overshadows any signal pulse.

In order to polarize the detector with only one voltage source, a voltage divider is used that distributes the source voltage between the anode and cathode and the negative and positive copper electrodes of each GEM foil, as illustrated in Figure 5. A capacitor (C1) located at the beginning of the divider circuit makes a low-pass filter and guarantees a clean DC voltage, and a second capacitor (C2) located at the end of the divider allows only detection of peak signals. This circuit was checked by applying a DC voltage of 4 kV. and measuring voltage and current at different points.

In Figure 5 we show the voltages within each GEM foil and the drift voltages between foils. The former cause the acceleration of electrons inside the holes of the GEM foil, while the latter make the electrons drift from one foil to the next. The values found are displayed in Table 1.

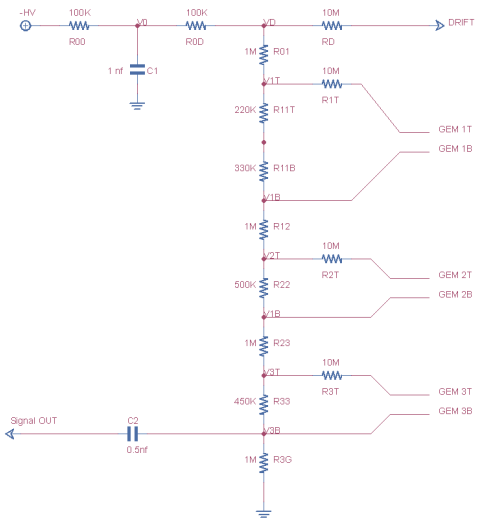

Figure 5. Voltage divider circuit for the triple-GEM detector (self-made).

Table 1. Voltages inside each GEM foil and between each drift region for the voltage divider circuit with a total source voltage of −4000 V.

Type		Voltage (V)
GEM voltages	VG1	-386.0
	VG2	-350.9
	VG3	-315.8
Drift voltages	VD1	-701.8
	VD2	-701.8
	VD3	-701.8

In order to test the performance of the detector, signals were taken with the oscilloscope for both cosmic muons and the Fe-55 radioactive source. Depending on the signal output used, the polarity was different. Pulses from the strips and from the bottom of the third GEM foil were measured to check the simultaneity of both outputs. We confirmed that every time it was triggered there was a signal on both channels. This means that we can make counts with either signal output. Most results have been done using the bottom of the third GEM foil output. The average Fe-55 signal is 8-10 mV. in height, and has a duration of 80 ns. The average muon signal is 1-10 mV. in amplitude, and a duration of 60-120 ns.

4.1 Optimal operating parameters

Supply voltage. In order to determine the optimal operating voltage, it was smoothly increased while registering counts, until sparks appeared in the detector.

Figure 6 presents these measurements for cosmic muons and for the Fe-55 source. The best operating voltage is about −4200 V, which is inside the plateau for the Fe-55 curve.

For muons it was impossible to reach the plateau. However, the muon count was verified using the known flux in Bogota, approximately 187 muons per minute [19].

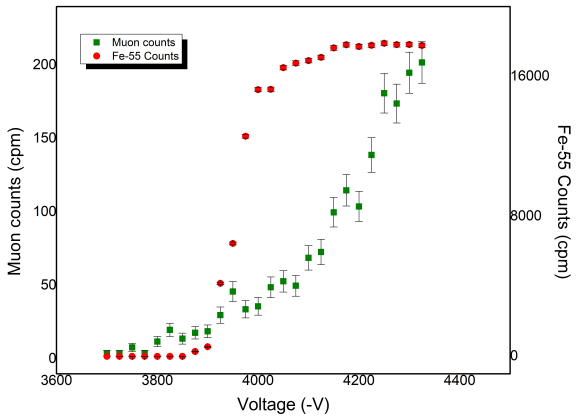

Figure 6. Counts vs Supply voltage for cosmic muons and the Fe-55 source. For muons, detections started at −3775 V and sparks at −4375 V. The expected value of 187 cpm was reached at around −4250 V. The efficiency is highest at the highest attained voltage before sparks occurred. For Fe-55, counts increase with voltage up to the efficiency plateau. The voltage of maximum efficiency is −4200 V, which lies in the middle of the plateau.

Threshold. Data was taken for counts vs. trigger threshold for muons at −4350 V. In Figure 7, it can be seen that above 1.3 mV noise is eliminated and the number of counts is stable, therefore the trigger threshold was chosen as 1.3 mV.

The same measurement was done for the Fe-55 source, where the appropriate trigger threshold was 2 mV.

Gas flow. Counts versus gas flow measurements were done with the Fe-55 source, increasing the gas flow from 0 to 0.55 l/min. The result is presented in Figure 8, where we can see a plateau above 0.25 l/min. Therefore, a gas flow of 0.3 l/min was chosen.

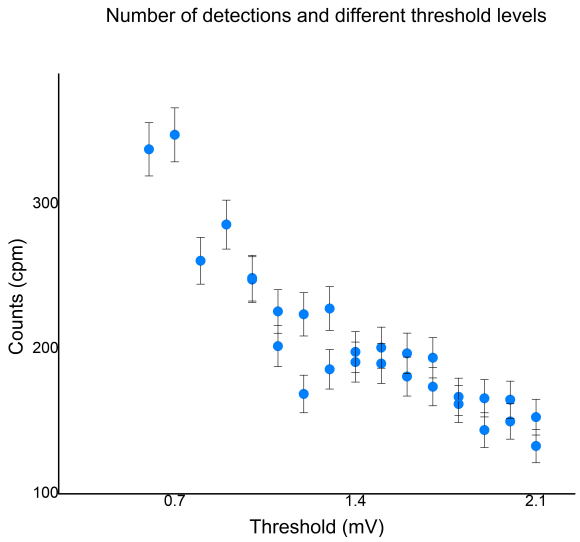

Figure 7. Counts vs Threshold for cosmic muons. At low thresholds there are high levels of noise. Above 1.3 mV counts tend to stabilize, therefore we chose this value as optimal threshold.

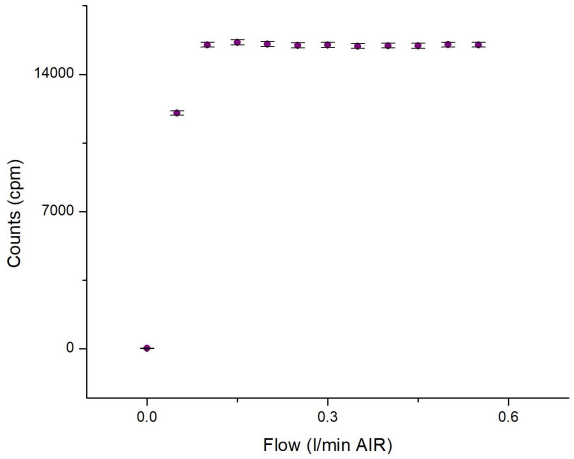

Figure 8. Counts vs Gas flow for the Fe-55 source. There is a plateau above 0.25 l/min, where the efficiency doesn't change with changes in gas flow. The optimal value of gas flow chosen was 0.3 l/min.

Table 2. Optimal operating parameters obtained for muons and the Fe-55 source.

Parameter	Muons	Fe-55
Supply voltage	-4325 V	-4200 V
Threshold	1.3 mV	2.0 mV
Gas flow	0.3 l/min	0.3 l/min

4.2 Energy resolution

The spectrum of the Fe-55 source was measured and after calibration we obtain the curve shown in Figure 9. We can observe two peaks: a tall one (the characteristic peak) at 5.9 keV, and the escape peak given by the energy of the emitted photoelectrons: $E_{p.e.} = E_\gamma - E_{K_\alpha} = 5.9 - 2.96 = 2.94$ keV [20].

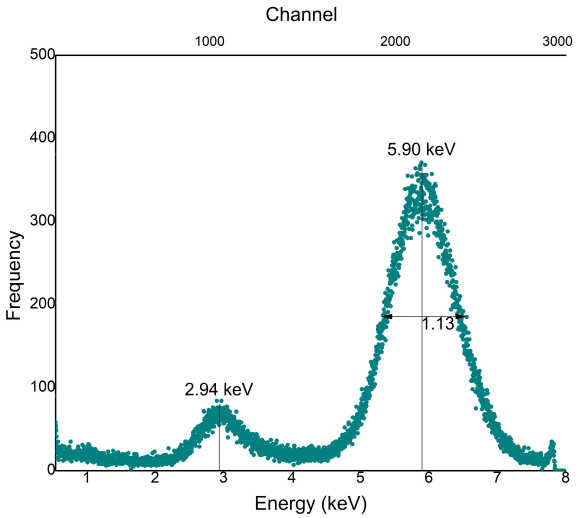

Figure 9. Spectrum of Fe-55. The small peak on the left is the argon escape peak, at 2.94 keV, and the peak on the right is the Fe-55 characteristic peak, at 5.9 keV. The latter has an FWHM of 1.13 keV.

In order to calculate the energy resolution, the FWHM was estimated by determining the maximum frequency, and subtracting the two average values of the spectrum at half of that frequency. This procedure gave an FWHM of 1.13 keV for the characteristic peak, which leads to the following energy resolution R:

$$R = \frac{\text{FWHM}}{E} = 0.195 \rightarrow 19.5\% \qquad (1)$$

where E is the position of the peak, 5.9 keV. This result agrees well with the value 20% reported in literature [21].

4.3 Time resolution

This measurement was made by directly observing in the oscilloscope the pulses generated in the detector by cosmic muons. The time resolution was obtained by measuring the width of the shortest muon pulses, giving 40 ns.

4.4 Linearity

Measurements were done with the Fe-55 source to check the linearity of the detector's response

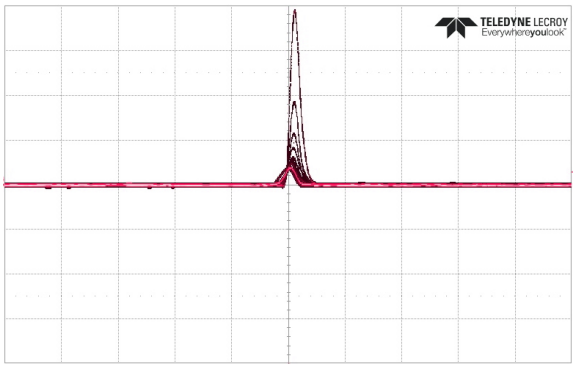

Figure 10. Muon persistence signals at a supply voltage of −4250 V. The horizontal time scale is 200 ns per division.

with radiation intensity, which was changed by interposing a different number of 0.016 mm thick aluminium sheets between the source and detector.

Figure 11 shows the results, where we can observe a linear dependence vs aluminum thickness in a logarithmic scale, confirming the linearity of the detector.

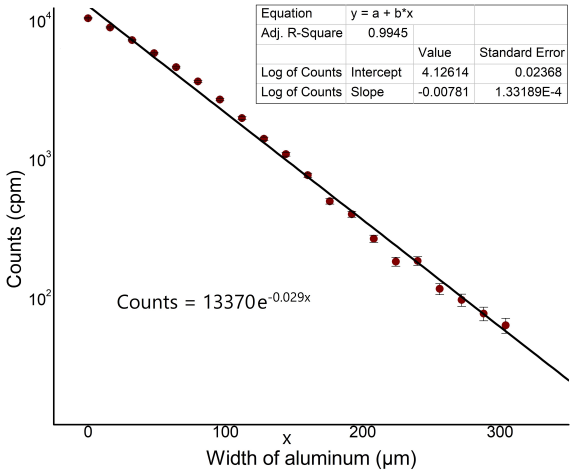

Figure 11. Counts vs Thickness of aluminum filters. It shows a linear response to X-ray photon beam intensity.

4.5 Efficiency

In order to determine the efficiency of the detector, counts of different radioactive sources were compared to the activity measured by the reference detector (Inspector EXP). The results are presented in Table 3. The triple-GEM detector has the best efficiency with the Fe-55 source. Although it has to be emphasized that the Inspector detector is not the most appropriate reference, since it was not made for all energies. The efficiency of the triple-GEM detector is low for low energy particles, since it was designed to count high energy muons. In particular, its efficiency for detecting electrons and alpha particles is remarkably low due to the attenuation produced by the Mylar window and structure of the top cathode.

Table 3. Efficiencies of the triple-GEM detector taking as reference the Inspector detector.

Source	Triple-GEM count (CPM)	Inspector count (CPM)	Triple-GEM efficiency
Fe-55	15,750	92,807	17.0%
Sr-90	11,155	232,500	4.80%
Tl-204	3,775	41,500	9.10%
Am-241	4,225	280,000	1.51%

4.6 Gain

In order to calculate the detector's gain the current was measured from the strips output, as a function of voltage, with the Fe-55 source placed on top at the center of the detector. The current without the radioactive source was subtracted from measured current values.

From the output current, gain can be calculated in the following way:

$$G = \frac{\text{collected charge}}{\text{primary charge}} = \frac{I}{f \cdot e \cdot n} \qquad (2)$$

where I is current, f is the number of detected particles that cross the detector per second, e is the elementary charge, and n is the number of primary electrons produced by a single incident particle. The detection factor was $f = 262 \pm 16$.

In order to calculate the number of primary electrons produced by 5.9 keV photons in the gas mixture used in the detector (Ar 75%-25% CO_2), checking the NIST tables, we verified that the photoelectric effect is the dominant process. Therefore, an absorbed energy of 5.9 keV can be assumed [22, 23], giving a number of primary electrons of $n = \frac{E_{Fe-55}}{W_{Ar-CO_2}} = \frac{5900\text{ eV}}{27.5\text{ eV}} \simeq 214$, where the mean ionization energy for the gas mixture is found in literature [12]. The gain vs supply voltage is shown in Figure 12.

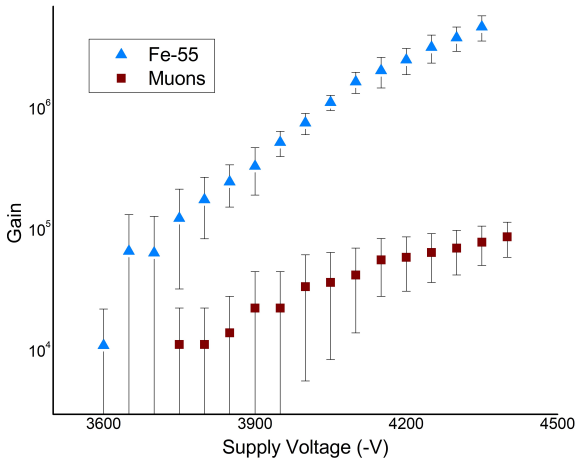

Figure 12. Gain vs Supply voltage with the Fe-55 source and with cosmic muons. The relationship is almost linear on a logarithmic scale, as expected in the proportional operating mode. The highest gain obtained was $(4.7 \pm 1.3) \times 10^6$.

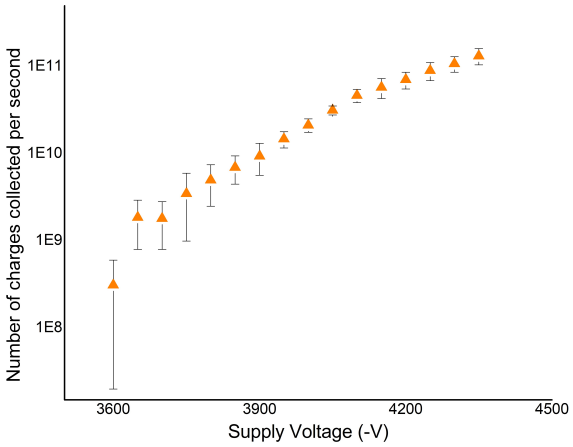

Figure 13. Characteristic curve of the detector. Number of charges collected per second vs Applied voltage with the Fe-55 source. This graph corresponds to the proportional counter region of the characteristic response curve for gaseous detectors. In this region, counts are proportional to the energy deposited by incoming particles.

We observe that gain presents an almost exponential dependence on supply voltage. The values are consistent with reported values [24], with a maximum gain of $(4.7 \pm 1.3) \times 10^6$. Measurements with cosmic muons gave similar results, also shown in Figure 12.

4.7 Characteristic response curve

The characteristic response curve is usually presented as collected charge vs. supply voltage on a logarithmic scale. The number of charges was determined from the measured current. The result for the Fe-55 source is presented in Fig. 13. As can be observed, in this scale the dependence is almost linear, which means that the detector is working in the **proportional counter region**, where counts are proportional to the energy deposited by incoming particles. This is satisfactory, not only because the gain is expected to be between 10^4 and 10^6, but also because in this operating region the absorbed dose can be calculated.

5 Conclusions and future work

The triple-GEM detector was assembled, characterized, and commissioned for future work. The following optimal operating parameters were found for cosmic muons: supply voltage: -4325 V, threshold voltage for pulse detection: 1.3 mV, and gas flow: 0.3 l/min. For the Fe-55 radioactive source: supply voltage: -4200 V., threshold voltage for detection: 2.0 mV, and gas flow: 0.3 l/min.

The following characteristic properties of the detector were obtained: energy resolution 19.5%, time resolution 40 ns, maximum gain $(4.7 \pm 1.3) \times 10^6$, and a greater count efficiency with cosmic muons than with any of the radioactive sources tested.

Advantages of the triple-GEM detector such as reaching high amplification factors at relatively low voltages, maintaining energy proportionality throughout its operating range, low noise, fast electronic signal, and ease of manipulation were demonstrated.

The detector has been characterized, commissioned, and calibrated in energy so that it can be used in studies of dosimetry, provided it is working in the proportional counter mode.

References

[1] L. Guirl, S. Kane, J. May, J. Miyamoto, and I. Shipsey, "An aging study of triple gems in Ar-CO2," *Nuclear Instruments and Methods in Physics Research Section A: Accelerators, Spectrometers, Detectors and Associated*

Equipment, vol. 478, no. 1-2, pp. 263–266, 2002.

[2] B. Ketzer, M. Altunbas, K. Dehmelt, J. Ehlers, J. Friedrich, B. Grube, S. Kappler, I. Konorov, S. Paul, A. Placci, et al., Triple gem tracking detectors for compass, IEEE Transactions on Nuclear Science 49 (5) (2002) 2403–2410.

[3] S. Lami, G. Latino, E. Oliveri, L. Ropelewski, N. Turini, T. Collaboration, et al., A triple-gem telescope for the totem experiment, Nuclear Physics B-Proceedings Supplements 172 (2007) 231–233.

[4] M. Poli Lener, L.-G. group, Triple-gem detectors for the innermost region of the lhcb muon apparatus, in: AIP Conference Proceedings, Vol. 794, American Institute of Physics, 2005, pp. 311–314.

[5] D. Abbaneo, M. Abbrescia, M. Abi Akl, C. Armaingaud, P. Aspell, Y. Assran, S. Bally, Y. Ban, P. Barria, L. Benussi, et al., Status of the triple-gem project for the upgrade of the cms muon system, Journal of Instrumentation 8 (12) (2013) C12031.

[6] G. D. D. CERN, https://gdd.web.cern.ch/, Gas Detectors Development Group at CERN.

[7] T. Behnke, R. Diener, C. Rosemann, L. Steder, A novel self-supporting gem-based amplification structure for a time projection chamber at the ilc, Journal of Instrumentation 8 (12) (2013) P12009.

[8] F. Simon, J. Kelsey, M. Kohl, R. Majka, M. Plesko, D. Underwood, T. Sakuma, N. Smirnov, H. Spinka, B. Surrow, Triple gem detectors for the forward tracker in star, in: 2007 IEEE Nuclear Science Symposium Conference Record, Vol. 1, IEEE, 2007, pp. 234–238.

[9] B. Azmoun, N. Smirnov, S. Stoll, C. Woody, Test of a gem detector in the phenix experiment at rhic, in: IEEE Symposium Conference Record Nuclear Science 2004., Vol. 1, IEEE, 2004, pp. 480–484.

[10] A. Velásquez and H. Castro, "Characterization and calibration of a Triple-GEM detector for medical dosimetry," *Nuclear Instruments and Methods in Physics Research Section A: Accelerators, Spectrometers, Detectors and Associated Equipment*, vol. 1000, p. 165241, 2021.

[11] D. N. Poenaru, W. Greiner, Experimental techniques in nuclear physics, Walter de Gruyter, 2011.

[12] W. Leo, *Techniques for nuclear and particle physics experiments: a how-to approach*. Springer Science & Business Media, 2012.

[13] D. Coy, "Construcción y caracterización de un detector de partículas tipo resistive plate chamber," Master's thesis, Universidad Nacional de Colombia, 2014.

[14] E. Rozo, "Desarrollo de un detector de rayos X y electrones para uso en radioterapia," Master's thesis, Universidad Nacional de Colombia, 2010.

[15] F. Murtas, "Development of a gaseous detector based on gas electron multiplier (GEM) technology," 2002, national Laboratory of Frascati, Istituto Nazionale di Fisica Nucleare.

[16] F. Sauli, "GEM: A new concept for electron amplification in gas detectors," *Nuclear Instruments and Methods in Physics Research Section A: Accelerators, Spectrometers, Detectors and Associated Equipment*, vol. 386, no. 2-3, pp. 531–534, 1997.

[17] F. Sauli, "The gas electron multiplier (GEM): Operating principles and applications," *Nuclear Instruments and Methods in Physics Research Section A: Accelerators, Spectrometers, Detectors and Associated Equipment*, vol. 805, pp. 2–24, 2016.

[18] J. Wang, Upgrade plans and ageing studies for the cms muon system in preparation of hl-lhc, arXiv preprint arXiv:1809.01760 (2018).

[19] J. Useche, C. Avila, Estimation of cosmic-muon flux attenuation by monserrate hill

in bogotá, arXiv preprint arXiv:1810.04712 (2018).

[20] B. Dorney, "Gas detector physics: Principles and fundamentals," May 2018.

[21] L. Cruz, "Caracterización y prueba de la cámara de ionización Triple-GEM a partir de muones resultantes de rayos cósmicos," Master's thesis, Universidad de los Andes, 2014.

[22] R. N. Patra, R. N. Singaraju, S. Biswas, Z. Ahammed, T. K. Nayak, and Y. P. Viyogi, "Measurement of basic characteristics and gain uniformity of a triple GEM detector," *Nuclear Instruments and Methods in Physics Research Section A: Accelerators, Spectrometers, Detectors and Associated Equipment*, vol. 862, pp. 25–30, 2017.

[23] M. Zecchin, "Characterization of a Triple-GEM detector prototype for the CMS muon spectrometer upgrade with gem detectors," Tech. Rep., 2014.

[24] S. Han, Y. Kim, J. M. Han, Y. S. Cho, Y. J. Kim, K. Jeong, H. Rang, D. H. Kim, H. Cho, S. Kang *et al.*, "Performance of a double GEM and a triple GEM," *Journal of the Korean Physical Society*, vol. 42, no. 5, pp. 606–611, 2003.